ELSEVIER

Catalysis Today 28 (1996) 31-39

CATALYSIS TODAY

The acidity of niobic acid studied by ^1H broad-line NMR at 4 K and ^1H MAS NMR at room temperature: comparison with other solid acids

Patrice Batamack *, Robert Vincent, Jacques Fraissard

Laboratoire de Chimie des Surfaces, associé au CNRS, URA 1428, Université Pierre et Marie Curie, Tour 55, 4 Place Jussieu, 75252 Paris Cédex 05, France

Abstract

The acidity of niobium pentoxide calcined at 573 K has been studied by interacting water molecules and the solid acid using ^1H broad-line NMR at 4 K and MAS NMR at room temperature. ^1H Broad-line NMR in 'rigid lattice' conditions allows the determination of the numbers of the oxygen–protonated species (H_3O^+ and $H_2O \cdots HO$ species, unreacted OH groups or excess H_2O molecules) present when water molecules used as base react with a Brønsted acid. With niobic acid, the method showed a continuous increase in the hydronium ion concentration with the number of water molecules. The ionization coefficient, determined when the ratio of the number of water molecules to that of the acidic hydroxyl groups of niobic acid is one, is 0.2. This value is similar to the ionization coefficients found for some HY zeolites.

Keywords: Niobic acid; NMR; Solid acids

1. Introduction

The acidity scale based on the Brønsted theory in the homogeneous phase, particularly in aqueous solution, has proved to be a fundamental tool in synthetic and applied chemistry. Despite numerous methods for investigating the acidity of solids, no universal acidity scale has been established for these compounds. The heterogeneity of solids and the poor knowledge of their surface do not facilitate the study of these materials [1]. The fundamental concept behind the Brønsted theory is the transfer of protons from the acid to the base. That clearly reveals that the acidity of a substance can only be evaluated in the presence of a base. The choice of a base is very important in the heterogeneous phase, since, some acidic sites may not be accessible. Using water molecules as the base satisfies many requirements. The molecule is small enough to access all acid sites and its hardness is convenient. Reactions with water are quantitative and in most cases equilibrated. Moreover, the species formed can be easily identified and their concentration determined.

Broad-line proton NMR at low temperature, generally at 4 K, has proved to be an interesting and powerful method for studying the surface of Brønsted acid solids interacting with small amounts of water [2]. This technique has made it possible to establish an acidity scale when

---

* Corresponding author.

SSDI 0920-5861(95)00216-2

equal numbers of acid sites and water molecules interact. The acidity scale proposed is limited to certain solids. The aim of this study is to enlarge this acidity scale to niobium pentoxide which presents a particular acid strength in the presence of water molecules [3].

Niobium supported on certain oxides has shown a remarkable promoter effect for various reactions [4] and niobium pentoxide treated at relatively low temperatures, T_t ($423 \leq T_t \leq 573$ K) is an effective catalyst for various reactions [5–8]. Sen et al. [9,10] have investigated the nature and structure of niobic acid. They conclude that this solid treated at 423 K is an isopolyacid, and from analytical results it can be written as $H_8Nb_6O_{19}$. On the basis of broad-line ^{1}H NMR quantitative analysis in the $573 \leq T_t \leq 1273$ K range, these authors state that the polymeric oxide form can be represented as $H_2Nb_6O_{16}$. DTA and TG analysis show that niobium pentoxide hydrate is completely dehydrated by heating to 573 K [5].

The surface acidity of niobic acid has been studied by n-butylamine titration using Hammett indicators, infrared spectroscopy of adsorbed pyridine [5,11] and by volumetric and gravimetric analysis of adsorbed NH_3 [12]. The surface of $Nb_2O_5 \cdot xH_2O$ contains both Lewis and Brønsted acid sites [5,13]. Iizuka and coworkers showed that for niobic acid, treated at $373 \leq T_t \leq 573$ K, there is a large number of acid sites having an acid strength, H_0, of -5.6. Infrared spectroscopy of adsorbed pyridine reveals that the pyridinium ion band intensity at 1540 cm^{-1} is highest when $T_t = 373$ K. When $T_t = 573$ K this band almost disappears while the bands of pyridine coordinately bonded to the surface, at 1610, 1480 and ca. 1446 cm^{-1}, are still present. This last band is strongest for niobic acid activated at 573 K. Niobic acid calcined at $773 \leq T_t \leq 873$ K is almost catalytically inactive although ^{1}H NMR quantitative analysis indicates that niobium oxide still contains two hydroxyl groups at $T_t \leq 1273$ K [9]. The surface acidity of niobium oxide depends on the preparation method and conditions [14]. Ushikubo and coworkers have studied the factors affecting the acid strength of niobic acid and have been able to prepare niobic acid with an H_0 of -8.2. Sulfation and phosphation resulted in a significant increase of the acidity of niobium oxide [11,12]. Guo and Qian [15] showed that crystallized niobic acid possesses more acid sites with higher strength than uncrystallized, sulphated or phosphated niobic acid.

We will report the study of the acidity of niobic acid using proton NMR techniques and in comparison with HY zeolites and other oxides.

2. Experimental

Niobium pentoxide hydrate, $Nb_2O_5 \cdot xH_2O$ (Niobia HY-340 AD/1123 from CBMM Laboratory, Brazil) was provided by Nissho Iwai Corporation, Japan. The surface area of the sample treated at 573 K, measured by nitrogen adsorption at 77 K, is 158 m^2 g^{-1}. The desorption process presents a hysteresis produced by mesopore effects. The pore distribution shows that the mean radius of the mesopores is 22 Å. About 0.6 g of sample in a glass ampoule were evacuated at room temperature to 10^{-2} Pa, then heated at a rate of 24 K h^{-1} up to 573 K and held at this temperature for at least 2 h. The number of protons on the calcined sample was determined from the ^{1}H MAS NMR spectrum by measuring the area under the curve, including the sidebands, and using distilled water as the absolute reference. The number of protons per gram of sample is 1.6×10^{21}. By comparing this number with the theoretical number of protons per gram of $H_2Nb_6O_{16}$, 1.5×10^{21}, we conclude that niobic acid evacuated at 573 K contains two hydroxyl groups, confirming the results of Ref. [9].

The NH_4Y zeolites for comparison were provided by UOP. The non-dealuminated zeolite, denoted NDY, after thermal treatment contains 47.7 bridging OH groups per unit cell, residual

Na^+ cations and no silanols [16]. The dealuminated zeolite, denoted DY for the H-form, was dealuminated by an aqueous solution of $(NH_4)_2SiF_6$. DY contains 35.8 bridging OH groups and 1.5 silanols per unit cell [17]. The characteristics of the samples are shown in Table 1. The acidic form of the zeolite was obtained by pumping a 5 mm thick layer of powder (shallow bed conditions) at room temperature to 10^{-2} Pa, followed by activation under vacuum at a rate of 12 K h^{-1} up to 675 K and held at this temperature for 16 h.

For all samples, water vapour was introduced at a constant temperature of 300 K in several steps, at pressures much lower than saturation; the amount of water was determined gravimetrically. The sample was held at 373 K overnight to ensure homogeneous distribution of the adsorbed water molecules and then sealed in thin 5 mm o.d. NMR tubes.

^1H MAS NMR experiments at room temperature are performed on a Bruker MSL-400 spectrometer with a home-made 5 mm probe. The rotation frequency of the sealed tubes is 3500–4500 Hz. Chemical shifts are expressed with respect to liquid TMS as external reference using the usual conventions.

The broad-line ^1H NMR spectra were recorded at 4 K on a home-made continuous wave 60 MHz spectrometer with phase detection and signal accumulation. The spectra are absorption derivatives. They are theoretically symmetrical with respect to the centre and, in practice, the two parts of each experimental spectrum are averaged; for this reason we show only half of each spectrum. In both cases, ^1H MAS and broad-line NMR, the weak residual signal of the probe is subtracted from the total signal.

The simulated spectra of broad-line ^1H NMR spectra correspond to the weighted sum of the oxyprotonated species involved and for which magnetic configurations are calculated [18–23]. (i) H_2O, an r-distant 2-spin configuration; (ii) H_3O^+, a magnetic configuration with three r-distant spins at the vertices of an equilateral triangle; (iii) $H_2O \cdots HO$ or distorted H_3O^+, a magnetic configuration with 3 spins at the vertices of an isosceles triangle, where r is the base and r' the equal sides; (iv) OH, a 2-spin configuration or a pure Gaussian and/or a pure Lorentzian function. Each of the corresponding functions (except the Gaussian and the Lorentzian ones) is convoluted by a Gaussian which takes into account the interaction between the protons of the configuration and those belonging to neighbouring configurations and also those of the non-zero spin nuclei in the environment (^{93}Nb or ^{27}Al). When the effect of these non-zero spins is small the parameter of each Gaussian is related to a distance X, which is close to the shortest distance between a proton of the configuration considered and a proton outside it. The numerical base takes into account the total number of protons in the sample, which is equal to the number of hydroxyl groups plus twice the number of water molecules introduced. Since, the number of independent parameters for each simulation is high, certain constraints are applied. We impose the condition that the water molecules introduced do not dissociate to produce additional OH groups. In

Table 1
Characteristics of niobic acid treated at 573 K and of anhydrous non-dealuminated (NDY) and dealuminated (DY) HY zeolites

Sample	Preparation (NMR)	Si/Al Na^+ per unit cell	OH per unit cell	$[Nb_6O1_6]^{2-}$ or 'anhydrous' zeolite	
				Acidic OH	Silanols
Niobic acid	'HY-340' from CBMM	–	–	2	–
NDY	'Y64' from UOP	2.4	8.3	47.7	0
DY	$(NH_4)_2SiF_6$	4.4	Negligible	35.8	1.5

addition, the distances r found must lie in the range corresponding to the various oxygen–proton species identified; this is always the case. For each configuration the value of X must be greater than (or at least equal to) that of r and r'.

In the following the concentrations, n_i, of the species adsorbed (H_2O) or formed (H_3O^+, $H_2O \cdots HO$) will be expressed relative to either the unit cell (n_i/uc) or per Brønsted acid site (n_i/bas).

3. Results

3.1. Niobic acid

3.1.1. ^1H MAS NMR at 300 K

The ^1H MAS NMR spectra are shown in Fig. 1. The spectrum of the anhydrous sample (Fig. 1a) presents two signals, one at 2.9 ppm, 1120 Hz wide at half-height, and a small broad shoulder at around 8 ppm with strong sidebands. The number of protons per gram of this sample is 1.6×10^{21}. Upon hydration, the exchange signal appears. The chemical shift of this signal varies from 6.4 ppm for $H_2Nb_6O_{16} \cdot 1H_2O$ (Fig. 1c) to 5.1 ppm for the fully hydrated sample, $H_2Nb_6O_{16} \cdot 10.6H_2O$ (Fig. 1f). At the same time, the width of the signal at half-height decreases from 4.6 to 1 KHz. A weak signal at 1.5 ppm is also observed at low hydration (Fig. 1b) but not in samples containing more than one water molecule per $H_2Nb_6O_{16}$ unit.

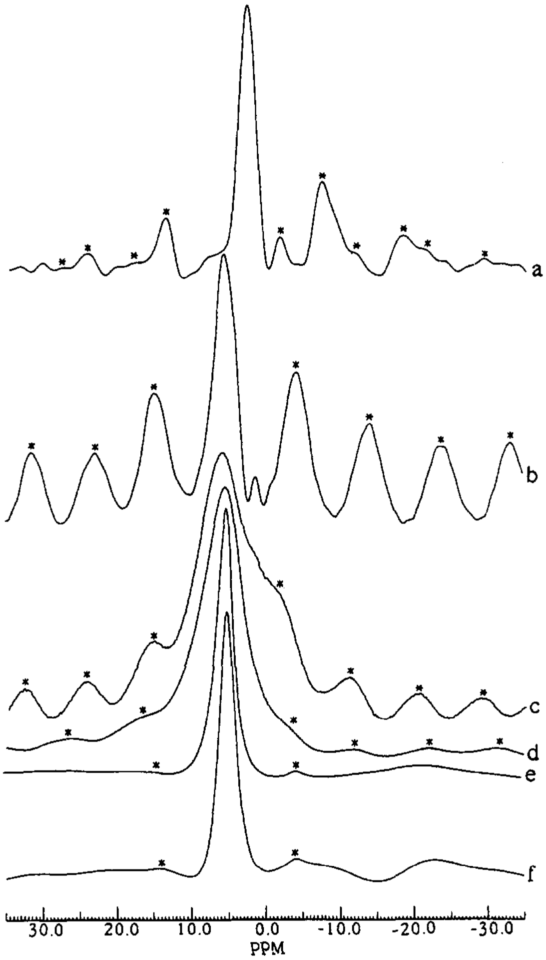

Fig. 1. ^1H MAS NMR spectra of niobium oxide samples: non-loaded niobium oxide, a; $H_2Nb_6O_{16} \cdot 0.27H_2O$, b; $H_2Nb_6O_{16} \cdot 1.06H_2O$, c; $H_2Nb_6O_{16} \cdot 2.3H_2O$, d; $H_2Nb_6O_{16} \cdot 4.8H_2O$, e; $H_2Nb_6O_{16} \cdot 10.6H_2O$, f; asterisks denote spinning sidebands.

3.1.2. ^1H broad-line NMR at 4 K

Fig. 2 shows the variation of some 4 K broad line ^1H NMR spectra with increasing water concentration: $H_2Nb_6O_{16} \cdot 0.54H_2O$, $H_2Nb_6O_{16} \cdot 2.3H_2O$ and $H_2Nb_6O_{16} \cdot 4.8H_2O$. The shape of the spectrum depends significantly on the water content. The spectrum of the anhydrous sample, not shown here, is poorly resolved and the fit is achieved with a two-spin line describing the magnetic interaction of the hydroxyl groups of the sample. All the other spectra consist of three maxima (at about 1.7, 6 and 10.5–11 $\times 10^{-4}$ T) which are well resolved for low water loading. All the spectra indicates hydronium ions and $H_2O \cdots HO$ species. In addition to these two species the spectrum of sample $H_2Nb_6O_{16} \cdot 0.54H_2O$, presents the lines of hydroxyl groups (Fig. 2a). For the samples containing more than 2 water molecules per $H_2Nb_6O_{16}$, the signal of the acidic OH groups is no longer visible, but that of water molecules not interacting is observed (Fig. 2b and Fig. 2c). Table 2 summarizes the concentrations of the different oxyprotonated species obtained for each sample and Table 3 gives the distance parameters used to simulate the spectra. Fig. 3 shows that $n_{H_3O^+}$/bas increases monotonically in the water concentration range studied. It seems, nevertheless, that the H_3O^+ concentration tends to a constant value for n_{H_2O}/bas $\geq$ 5.3. The ionization coefficient is ca. 0.2 when n_{H_2O}/bas = 1 (the number of water molecules per acid site) and for n_{H_2O}/bas = 5.3 the ionization coefficient is 0.5.

3.2. *HY zeolites*

We will briefly recall the results of Y zeolites for the purpose of the discussion. Refs. [16] and [17] present the details of these results.

3.2.1. *^1H MAS NMR at 300 K*

The signals of acidic bridging OH groups pointing toward the sodalite cavities and the supercages characteristic of HY zeolites are present in the spectra of both anhydrous samples [24]. The signal of silanol groups detected for DY is negligible for NDY. Upon hydration a Lorentzian signal corresponding to chemical exchange between the oxyprotonated species (H_2O, bridging OH groups, and hydronium ions) is visible for both compounds. It is interesting to note that, in addition to the Lorentzian signal, there is a Gaussian signal at 6.5 ppm due to water on Lewis acid sites on the spectra of DY when the number of water molecules per acid site, n_{H_2O}/bas, is less than 1/3. This signal is no longer visible when n_{H_2O}/bas $\geq$ 1/3. It is probably hidden by the Lorentzian line which is at about 7 ppm and whose half-height is 1600 Hz when n is about 1. When n_{H_2O}/bas $\gg$ 1 the exchange signal shifts to low values of the chemical shift and the line-width is reduced. However, the 6.5 ppm Gaussian line observed at low water loadings is not present. There is a small signal at about 10 ppm for both samples when n_{H_2O}/bas $\gg$ 1. This signal is due to $[Al(H_2O)_6]^{3+}$ [25]. The number of hexacoordinated Al atoms is always less than 2 per unit cell. Very little dealumination always occurs when n_{H_2O}/bas > 1 in the rehydrated samples [26]. Dealumination is also favoured by homogenization of the samples.

3.2.2. *^1H broad-line NMR at 4 K*

Simulation of the spectra of both samples showed that when n_{H_2O}/bas < 1 all water molecules interact with the bridging OH groups to give hydronium ions and hydrogen-bonded species ($H_2O \cdots HO$). In this range the concentration of hydronium ions increases with the amount of adsorbed water. In the case of DY, in addition to 'free' acidic OH groups, a contribution of 3%–4% of silanol groups (in the anhydrous sample) not interacting with water molecules as shown by proton MAS NMR improves the simulations. For n_{H_2O}/bas = 1 no 'free' acidic groups are observed and the species identified are H_3O^+ and $H_2O \cdots HO$. At higher hydration levels there are 'free' water molecules.

Table 2
Number of oxygen-protonated species per $H_2Nb_6O_{16}$ unit after adsorption of the number of water molecules per $H_2Nb_6O_{16}$ unit

Number of adsorbed water molecules	Number of H_3O^+ ions	Number of $H_2O \cdots HO$ groups	Number of 'free' acidic OH groups	Number of water molecules
0.0	0.0	0.0	2.00 ± 0.20	0.0
0.54 ± 0.05	0.13 ± 0.02	0.43 ± 0.05	1.45 ± 0.16	0.0
1.06 ± 0.05	0.23 ± 0.03	0.82 ± 0.09	0.95 ± 0.09	0.0
2.3 ± 0.1	0.39 ± 0.05	1.57 ± 0.17	0.0	0.33 ± 0.04
3.8 ± 0.2	0.58 ± 0.07	1.47 ± 0.15	0.0	1.7 ± 0.2
4.8 ± 0.2	0.83 ± 0.09	1.18 ± 0.12	0.0	2.8 ± 0.3
7.6 ± 0.3	0.94 ± 0.09	1.06 ± 0.11	0.0	5.6 ± 0.5
10.6 ± 0.5	1.00 ± 0.10	1.00 ± 0.10	0.0	8.6 ± 0.8

For NDY, the concentration of H_3O^+ ions is almost constant from n_{H_2O}/bas = 1 to 3. The ionization coefficient is 0.2. Fig. 2 shows the dependence of $n_{H_3O^+}$/bas on n_{H_2O}/bas for NDY. For DY (Fig. 3), a plateau is observed when $1 \leq n_{H_2O}/\text{bas} \leq 2$. Here also, the ionization coefficient in the horizontal section is 0.2. The concentration of hydronium ions increases significantly when $n_{H_2O}/\text{bas} > 2$. For example, the ionization coefficient is 0.44 when n_{H_2O}/bas = 4.4.

4. Discussion

Zeolites present acidic hydroxyl groups at 4.5–5.5 ppm while niobic acidic hydroxyl groups are at 2.9 and ca. 8 ppm. Nevertheless, as has been already said, the chemical shift is not a measure of the acidity, since, it depends not only on the ionic character of the bond but also on the environment (influence of hydrogen bonds, for instance). Moreover, the acidity does not depend only on the ionic character of the OH bond but also on its polarisability in the presence of a proton-acceptor. After hydration, the mean chemical shift of the exchange signal between the proton of species present varies from about 5 to 7 ppm for the three compounds. At low water loadings, when $n_{H_2O}/\text{bas} < 1$ there is a signal at 1.5 ppm for niobic acid samples. This signal is masked by that of the acidic hydroxyl groups on the non-loaded sample and may be due to impurities. These hydroxyl groups represent about 4 per cent of the total number of protons in the $H_2Nb_6O_{16} \cdot 0.27H_2O$ sample.

The dependence of $n_{H_3O^+}$/bas on n_{H_2O}/bas is different for the three compounds (Fig. 3). The shape of these curves seems to be related to the nature of the defects and the structure of the compounds. DY contains defects evidenced by both ^1H and ^{129}Xe NMR experiments. The nature of these defects is not definitely identified and depends on how the sample is treated [27–29]. Batamack and coworkers showed that the defects in DY are probably tricoordinated aluminum partially bonded to the zeolite framework. These Lewis-type framework defects result from the treatment with a solution of ammonium hexafluorosilicate [29]. A possible mechanism explaining the increase in the number of hydronium ions when $n_{H_2O}/\text{bas} > 2$ was proposed. In the presence of two water molecules per Brønsted acid site, a network of hydrogen bonds between water molecules and connecting Brønsted and Lewis acid sites weakens the acidic OH bonds, which favours the formation of hydronium ions. Defects of a different nature in some MFI and mordenite zeolites show similar behaviour to those in DY [30,31]. For niobic acid, the concentration of H_3O^+ ions increases continuously with the concentration of adsorbed water molecules at least,

Table 3
Distance parameters (in pm) used for simulation of $H_2Nb_6O_{16} \cdot xH_2O$ spectra

No. of adsorbed water molecules per $H_2Nb_6O_{16}$ unit	Hydroxonium ions (isosceles symmetry)			$H_2O \cdots HO$ groups			Acidic OH groups		H_2O molecules	
	$r \pm 2$	$r' \pm 5$	$X \pm 5$	$r \pm 2$	$r' \pm 5$	$X \pm 5$	$r \pm 2$	$X \pm 5$	$r \pm 2$	$X \pm 5$
0.54 ± 0.05	162	167	218	164	258	265	195	195		
							Gaussian	244		
1.06 ± 0.05	161	169	223	158	224	253	192	192		
2.3 ± 0.1	158	169	216	158	229	233			157	233
3.8 ± 0.2	158	169	216	158	229	233			157	204
4.8 ± 0.2	157	168	215	158	231	236			157	204
7.6 ± 0.3	156	167	220	157	229	240			158	198
10.6 ± 0.5	157	168	219	157	232	243			158	197

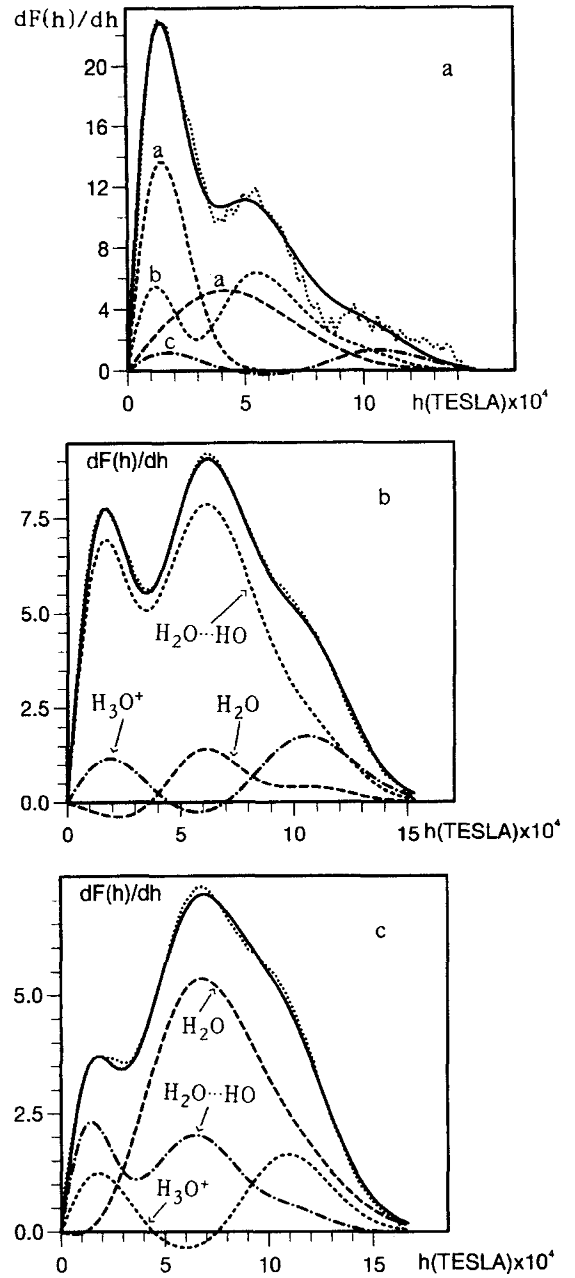

Fig. 2. a: Half derivative ^{1}H NMR broad-line spectrum of $H_2Nb_6O_{16}\cdot 0.54H_2O$ sample. (a) the weighted contributions of OH groups, (b) the weighted contributions of $H_2O\cdots HO$ species, (c) the weighted contribution of H_3O^+ ions, (· · ·) experimental and (—) fitted spectra. b: Half derivative ^{1}H NMR broad-line spectrum of $H_2Nb_6O_{16}\cdot 2.3H_2O$ sample. The weighted contribution of each oxygen-protonated species is shown on the spectrum. (· · ·) Experimental and (—) fitted spectra. c: Half derivative ^{1}H NMR broad line spectra of $H_2Nb_6O_{16}\cdot 7.6H_2O$ sample. The weighted contribution of each oxygen–protonated species is shown on the spectrum. (· · ·) Experimental and (—) fitted spectra.

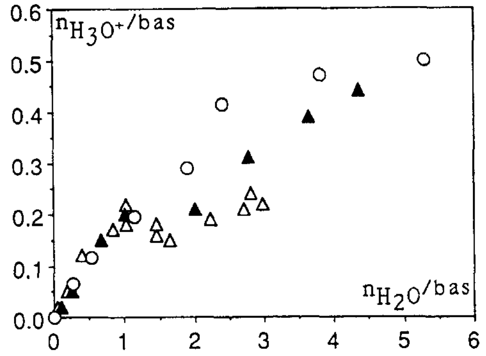

Fig. 3. Variation of $n_{H_3O^+}$/bas with adsorbed n_{H_2O}/bas for samples: ○ niobic acid, △ NDY and ▲ DY.

in the range studied. It appears that an asymptote is reached for $n_{H_2O}/\text{bas} \geq 5.3$. A first explanation consists in saying that the continuous increase in the number of H_3O^+ ions per acid site is due to dilution by the addition of water molecules. In fact, it is well known that in an aqueous solution the dilution of weak and medium electrolytes increases the ionization coefficient. A second explanation takes into consideration the fact that the surface acidity of hydrated niobium pentoxide treated at 573 K consists mainly of Lewis acid sites [5]. As in DY, the connection between Brønsted and Lewis acid sites through hydrogen bonds results in an increase in the hydronium ions concentration. The results of the simulation of the broad-line spectra (Table 1) show that the number of hydrogen-bonded species ($OH \cdots H_2O$) decreases while that of hydronium ions rises when the water concentration increases. Furthermore, in Table 2 the distance parameter, X, of water molecules diminishes when the water content of the sample is increased, proving the proximity of these molecules to the others. Let us recall that X is the average shortest distance between protons and/or other nuclei of distinct magnetic configurations. The plateau observed in DY when $1 < n_{H_2O}/\text{bas} < 2$ does not occur in niobic acid. This means that, according to this second hypothesis, the synergy between Brønsted and Lewis acids sites seems to be stronger in niobic acid. This may be favoured by the relative small surface area of niobic acid and, consequently, by the proximity of the acid sites.

The acidity scale, so far established using broad-line proton NMR, is on the basis of equal numbers of water molecules and Brønsted acid sites of the solid in interaction. When the acid strength of the hydroxyl groups of the solid is strong enough, dissociation occurs and the ionization coefficient can be determined from the concentrations of the different oxyprotonated species [2]. This is the case of DY and NDY zeolites and niobic acid. The higher the ionization coefficient, the stronger the acid. We found that for these compounds the ionization coefficient is ca. 0.2. This means that the mean acidities of the three compounds at this level of hydration are similar, but they are less acidic than H-ZSM-5 zeolite SiOH(Al) $\cdot$ H_2O (0.3), H-Mordenite zeolite SiOH(Al) $\cdot$ H_2O (0.33), $H_2Sb_4O_{11} \cdot 2H_2O$ (0.4), sulphated zirconia (0.5) and Nafion-H $\cdot$ H_2O (1) [2]. The numbers in brackets represent the ionization coefficients.

This method is so powerful that it can even differentiate solid acids when dissociation does not occur. In this case, only the species in which acidic OH groups hydrogen-bonded to adsorbed water molecules ($OH \cdots H_2O$ species) are formed. We have to bear in mind that the direct dipolar magnetic interaction is proportional to $1/r^3$, where r is the distance between two neighbouring protons. This means that the technique is very sensitive to the geometry of the species. We can, therefore, determine with accuracy the H–H distances in the proton magnetic configurations and deduce the hydrogen bond strength. Here also, solid acids are compared when $n_{H_2O}/\text{bas} = 1$, assuming the O–H distance in the solid is 100 pm. The shorter the hydrogen bond, the greater the acid strength. Table 4 shows the acidity scale of solids, including cases when dissociation occurs or not, and that of OH groups not interacting with water molecules (silanol groups in zeolites).

5. Conclusion

Room temperature ^1H MAS NMR and 4 K broad-line NMR study of the surface acidity of hydrated niobium pentoxide treated at 573 K show that the number of hydroxyl groups on the anhydrous sample is low (2 H atoms per $[Nb_6O_{16}]^{2-}$). The variation of hydronium ion concentration with the number of adsorbed water molecules is different for niobic acid, dealu-

Table 4
Acidity scale of some solids

Sample	Number of H_3O^+ per initial OH: ionization coefficient	Number of $H_2O \cdots HO$ per initial OH	r (pm)	r' (pm)	O–O (pm) distance from r and r'; $H_2O \cdots O$ assumed C_{2v}
Sulfated zirconia (second acidity)	0	0			
Zeolite silanols	0	0			
Superficial OH groups on amorphous TiO_2	0	1	143	265	285
$H_2AlP_3O_{10} \cdot 2H_2O$	0	1	163	216	242
HY zeolite SiO(H)Al	0.2	0.8	162	232	259
Niobic acid			158	169	188
H-ZSM-5 zeolite SiO(H)Al	0.3	0.7	163	236	276
H-mordenite SiO(H)Al	0.33	0.67	165	247	263
$H_2Sb_4O_{11} \cdot 2H_2O$	0.4	0.6	164	221	247
Sulfated zirconia (mean acidity)	0.5	0			
Nafion	1	0			
Sulfated zirconia (first acidity)	1	0			

minated HY zeolite (DY) and HY zeolite without defects (NDY). For niobic acid, $n_{H_3O^+}$ increases monotonically with n_{H_2O}. For DY, there is a gradual increase until the number of water molecules per Brønsted acid site, n_{H_2O}/bas, equals 1; it is then constant when $1 < n_{H_2O}/\text{bas} \leq 2$ and for $n_{H_2O}/\text{bas} > 2$, the number of hydronium ions increases significantly. For NDY, the situation is similar to DY when $n_{H_2O}/\text{bas} \leq 1$ but, when $n_{H_2O}/\text{bas} > 1$ the number of H_3O^+ ions is almost constant. These differences are attributed to the combined effect of dilution and the synergy between Brønsted and Lewis acid sites present in niobic acid and DY. The dilution factor by itself is not sufficient to weaken the acidic OH groups and increase the ionization coefficient. This seems to happen for the NDY without defects. Only weak hydrogen bonds are formed between water molecules. When $n_{H_2O}/\text{bas} = 1$, the ionization coefficient is ca. 0.2 for all three compounds; at this water content, the acidities of these compounds are similar. According to the broad-line ^{1}H NMR results, at full hydration 50% of the acid sites of niobic acid are ionized, revealing that only one of the two acid sites of niobium oxide is particularly strong. This behaviour is similar to that of diprotic acids in solution.

Acknowledgements

We are grateful to CBMM Laboratory of Brazil and the Nissho Iwai Corporation of Japan for providing us with the hydrated pentoxide sample and to UOP for the zeolite samples. We thank Professor Kozo Tanabe for his great help and encouragement.

References

[1] K. Tanabe, Solid Acids and Bases, Kodansha, Tokyo, Academic Press, New York, 1970.

[2] P. Batamack, C. Dorémieux-Morin, R. Vincent and J. Fraissard, J. Phys. Chem., 97 (1993) 9779.

[3] P. Batamack, R. Vincent and J. Fraissard, Catal. Lett, submitted for publication.

[4] K. Tanabe, Catal. Today, 8 (1990) 1.

[5] T. Iizuka, K. Ogasawara and K. Tanabe, Bull. Chem. Soc. Jpn., 56 (1983) 2927.

[6] Z. Chen, T. Iizuka and K. Tanabe, Chem. Lett., (1984) 1085.

[7] K. Ogasawara, T. Iizuka and K. Tanabe, Chem. Lett., (1984) 645.

[8] T. Iizuka, S. Fujie, T. Ushikubo, Z. Chen and K. Tanabe, Appl. Catal., 28 (1986) 1.

[9] B.K. Sen, A.V. Saha and N. Chatterjee, Mater. Res. Bull., 16 (1981) 923.

[10] B.K. Sen and A.V. Saha, Mater. Res. Bull., 17 (1982) 161.

[11] S. Okazaki, M. Kurimata, T. Iizuka and K. Tanabe, Bull. Chem. Soc. Jpn., 60 (1987) 37.

[12] A. Kurosaki, T. Okuyama and S. Okazaki, Bull. Chem. Soc. Jpn., 60 (1987) 3541.

[13] K. Tanabe, M. Misono, Y. Ono and H. Hattori, Stud. Surf. Sci. Catal., 51 (1989) 61.

[14] T. Ushikubo, T. Iizuka, H. Hattori and K. Tanabe, Catal. Today, 16 (1993) 291.

[15] C. Guo and Z. Qian, Catal. Today, 16 (1993) 379.

[16] P. Batamack, C. Dorémieux-Morin and J. Fraissard, J. Chem. Phys., 89 (1992) 423.

[17] P. Batamack, C. Dorémieux-Morin and J. Fraissard, Catal. Lett., 11 (1991) 119.

[18] G.E. Pake, J. Phys. Chem., 16 (1948) 327.

[19] E.R. Andrew and R.J. Bersohn, J. Phys. Chem., 18 (1950) 159.

[20] R.E. Richards and J.A.S. Smith, Trans. Faraday Soc., 48 (1952) 675.

[21] E.R. Andrew and N.D. Finch, Proc. Phys. Soc., 70B (1957) 980.

[22] C. Dorémieux-Morin, J. Magn. Reson., 21 (1976) 419.

[23] A.L. Porte, H.S. Gutowsky and J.E. Boggs, J. Phys. Chem., 36 (1962) 1695.

[24] D. Freude, M. Hunger, H. Pfeifer, G. Scheler, J. Hoffmann and W. Schmitz, Chem. Phys. Lett., 105 (1984) 427.

[25] J.W. Akitt, J.M. Elders and X.L.R. Fontaine, J. Chem. Soc., Chem. Comm., (1986) 1047.

[26] L.M. Parker, D.M. Bibby and G.R. Burns, Zeolites, 11 (1991) 293.

[27] D. Freude, Chem. Phys. Lett., 235 (1995) 69.

[28] D. Freude, M. Hunger and H. Pfeifer, J. Chem. Soc., Faraday Trans., 87 (1991) 657 and references therein.

[29] P. Batamack, C. Dorémieux-Morin, R. Vincent and J. Fraissard, Microporous Mater., 2 (1994) 515.

[30] P. Batamack, C. Dorémieux-Morin and J. Fraissard, Proc. 10th Int. Cong. Catal., (1992) 243.

[31] L. Heeribout, V. Semmer, P. Batamack, C. Dorémieux-Morin, R. Vincent and J. Fraissard, Trans. Faraday Soc., submitted for publication.